



Cite this: *RSC Adv.*, 2019, 9, 8073

# A porous $\beta$ -cyclodextrin-based terpolymer fluorescence sensor for *in situ* trinitrophenol detection†

Michael K. Danquah,<sup>a</sup> Shan Wang,<sup>b</sup> Qianyou Wang,<sup>b</sup> Bo Wang <sup>\*b</sup> and Lee D. Wilson <sup>\*a</sup>

Permanent porosity plays a key role in fluorescent-based polymers with “on–off” emissive properties due to the role of guest adsorption at accessible fluorophore sites of the polymer framework. In particular, we report on the design of a porous fluorescent polymer (FL-PFP) composed of a covalently cross-linked ternary combination of  $\beta$ -cyclodextrin ( $\beta$ -CD), 4,4'-diisocyanato-3,3'-dimethyl biphenyl (DL) and tetrakis(4-hydroxyphenyl)ethene (TPE). The textural properties of FL-PFP were evaluated by the gas uptake properties using  $N_2$  and  $CO_2$  isotherms. The BET surface area estimates according to  $N_2$  uptake ranged from 100–150  $m^2 g^{-1}$ , while a lower range of values (20–30  $m^2 g^{-1}$ ) was estimated for  $CO_2$  uptake. Model nitroarenes such as trinitrophenol (TNP) and nitrobenzene (NB) were shown to induce turn-off of the fluorescence emission of the polymer framework at concentrations near 50 nM with ca. 50% fluorescence quenching upon TNP adsorption and detection. The strong donor–acceptor interaction between the nitroarenes and the TPE reporter unit led to fluorescence quenching of FL-PFP upon nitroarene adsorption. The fluorescence lifetime ( $\tau$ ) for FL-PFP ( $\tau = 3.82$  ns) was obtained along with a quantum yield estimate of 0.399 relative to quinine sulphate. The  $\beta$ -CD terpolymer reported herein has significant potential for monitoring the rapid and controlled detection of nitroarenes (TNP and NB) in aquatic environments and other complex media.

Received 22nd July 2018  
Accepted 28th February 2019

DOI: 10.1039/c8ra06192k

rsc.li/rsc-advances

## Introduction

Trinitrophenol (TNP) and nitrobenzene (NB) are deleterious nitroarene compounds that have manifold utility for the chemical synthesis of dyes, pesticides and as additives in incendiary devices. The ubiquitous presence of nitroarenes in various industrial processes have led to concerns over human exposure and environmental contamination due to their known toxicity, along with their variable fate and transport in aquatic environments.<sup>1–3</sup> To address the environmental concerns related to the build-up and transport of nitrophenols, research activity has been directed toward the selective and sensitive detection of model compounds such as TNP and NB. Analytical detection and quantification methods such as X-ray dispersion, surface-enhanced Raman spectroscopy<sup>4</sup> IR spectroscopy<sup>5</sup> and mass spectrometry<sup>6</sup> have been reported. However, considerations of

analysis time and cost of such techniques have limited their application for field studies. By contrast, fluorescence detection methods have gained increasing interest owing to their cost-effectiveness, high sensitivity and their relatively facile operation.<sup>6–9</sup> Although ultra-high sensitivity toward nitroarene explosives are known, challenges remain concerning their rapid and selective detection with the use of conventional sensors in the field. Fluorescence-based sensors have been developed for the selective and sensitive detection of model explosive materials that use various modalities of detection that include fluorescent quantum dots,<sup>10,11</sup> fluorescence immunoassays<sup>12–14</sup> and colorimetric visualization methods.<sup>15</sup> Despite the advantages of these methods in the field of nanotechnology for the selective detection of model explosives, there is a need to develop fluorescence-based sensors with greater surface area and controlled uptake for the sorptive removal and selective detection of nitroarenes from aqueous media.

There are reports on the design of fluorescent framework materials for the detection of nitroarenes where luminescent metal–organic frameworks (MOFs) have been extensively studied due to their luminescent properties.<sup>9,16,17</sup> These systems are promising in light of the detection limit of nitroaromatic compounds that range between 6.5 nM to 100 nM.<sup>6,7,9,11,12,14,17,18</sup> While luminescent MOFs are known to provide good sensitivity and selectivity due to their porous nature and their favourable

<sup>a</sup>Department of Chemistry, University of Saskatchewan, 110 Science Place, Saskatoon, Saskatchewan S7N 5C9, Canada. E-mail: lee.wilson@usask.ca; Fax: +1-306-966-4730; Tel: +1-306-966-2961

<sup>b</sup>Beijing Key Laboratory of Photoelectric/Electrophotonic Conversion Material, Key Laboratory of Cluster Science, Ministry of Education, School of Chemistry and Chemical Engineering, Beijing Institute of Technology, 5 South Zhongguancun Street, Beijing 100081, P. R. China

† Electronic supplementary information (ESI) available. See DOI: 10.1039/c8ra06192k

host-guest complexation behaviour, organic polymer-based luminescent materials have also gained recent attention.<sup>19,20</sup> Zhao *et al.*<sup>20</sup> reported on conjugated polymers, poly(*p*-phenyleneethynylene)s (PPEs) and poly(*p*-phenylenebutadiynylene)s (PPDs) materials with unique detection of nitroarenes in solution and the solid state. Zhao *et al.*<sup>20</sup> also reported that the porosity of the polymer strongly affects the sensitivity of detection of the target compounds by providing variable surface functionality which favours detection. The role of porosity in polymer materials has been reported for cross-linked materials containing calixarenes, porphyrins, crown ethers and cyclodextrins.<sup>21</sup> These polymer systems can act as good receptors by forming stable complexes with nitroarenes and related pollutants by increasing the selectivity and sensitivity of the host material.<sup>21</sup>

Cyclodextrins (CDs) are unique supramolecular hosts due to their ability to form stable host-guest complexes with diverse types of inorganic and organic guest systems.<sup>22–30</sup> The moderate cost and solubility of  $\beta$ -CD has led to its utility in the design of polymer materials, where the host-guest chemistry of the polymer compares favourably with that of the native CD. However, CD-based polymers are known to display unique adsorption properties due to the occurrence of dual mode binding at the inclusion and interstitial sites of the polymer framework.<sup>25</sup> Recent reports indicate that  $\beta$ -CD-based polymers with high surface area and variable rigidity<sup>31,32</sup> adsorb pollutants with higher affinity due to their greater surface area and pre-organized binding sites. The development of advanced  $\beta$ -CD-based materials like green CD-MOFs and CD-based sensors have been reported by Wang *et al.*,<sup>16,17</sup> where a CD-based polymer was used to indirectly determine fluorescent BPA in solution *via* the formation of host-guest complexes. In this study, the CD inclusion sites were attributed to the fluorescence detection of BPA while the interstitial binding sites were unaccounted for in the mechanism of fluorescence detection. A recent review has suggested that CDs show promise as luminescent sensors due to the role of host-guest complexation and molecular self-assembly.<sup>21</sup> Tanabe *et al.*<sup>33</sup> reported on the use of dansyl-glycine-CDs immobilized onto cellulose for the fluorescence detection of 1-adamantanol, where the dansyl group may undergo self-assembly or inclusion within the CD cavity.<sup>21</sup> Liang *et al.*<sup>34</sup> reported on the fluorescence detection of volatile organic compounds (VOCs) by formation of host-guest complexes of CDs with tetraphenylethene (TPE) units. A moderate detection limit was achieved for such VOCs ( $5 \mu\text{g L}^{-1}$ ). However, the utility of the approach appears limited due to the requirement of VOCs transfer to the solution phase that may have thermodynamic and kinetic mass transfer limitations due to gas solubility in water by Henry's law.

Fluorescence species that display on-off luminescence behaviour in the aggregated state or in the solid phase may relate to aggregation induced emission (AIE) or aggregation induced quenching (AIQ) that arise due to restriction in the intramolecular rotations of fluorescent molecules.<sup>35–37</sup> TPE systems belong to a group of fluorophores that exhibit AIE effects and have been recently exploited due to the enhanced luminescence properties in their molecular and other cross-linked forms.<sup>38,39</sup> Recent studies have reported on the enhanced selectivity and sensitivity of TPE macrocyclic

compounds and TPE cross-linked polymers for the detection of explosives.<sup>40</sup>

Herein, we report on the characterization and the application of a porous fluorescent polymer derived from coupling  $\beta$ -CD with 4,4'-diisocyanato-3,3'-dimethylbiphenyl (DL) and tetrakis(4-hydroxyphenyl)ethane (TPE) to form a cross-linked polymer (FL-PFP). The fluorescence detection of TNP or NB with FL-PFP according to the formation of complexes (FL-PFP/TNP and FL-PFP/NB) were studied in aqueous solution using fluorescence spectroscopy. This work demonstrates the general utility and the design features of FL-PFP that contribute to its molecular recognition of nitroarene guest systems. As well, this research demonstrates that sensor materials with permanent porosity *via* cross-linking of TPE with  $\beta$ -CD affords controlled sorption and *in situ* detection of nitroarene guest systems.

## Experimental

### Materials

$\beta$ -Cyclodextrin ( $\beta$ -CD;  $\geq 99\%$ ), 4,4'-diisocyanato-3,3'-dimethylbiphenyl (DL), *N,N'*-dimethylacetamide (DMA), dimethylformamide (DMF), tetrakis(4-hydroxyphenyl)ethane (TPE), 2,4,6-trinitrophenol (TNP), nitrobenzene (NB), Tris-HCl and acetone were obtained from Beijing Chemical Reagent Company.

### Synthesis of fluorescent-based polymer (FL-PFP)

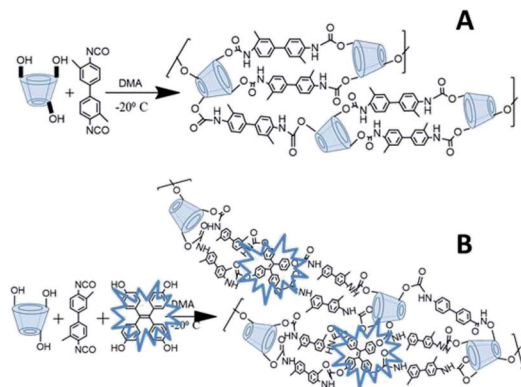
$\beta$ -CD (0.185 g, 0.162 mmol) was purged with  $\text{N}_2$  for 5 min, where 5 mL DMA was added to the mixture with equilibration at  $-20^\circ\text{C}$  for 30 minutes. DL (0.435 g, 1.64 mmol) was pre-dissolved in 5 mL of DMA and then added to the mixture over 20 min, followed by addition of TPE (0.128 g, 0.324 mmol) with stirring for 48 h. A creamy brown suspension was formed and the brown solids were washed with distilled water ( $3 \times 10 \text{ mL}$ ). Subsequent washing with DMF ( $3 \times 10 \text{ mL}$ ), acetone ( $3 \times 10 \text{ mL}$ ) and finally with distilled water ( $3 \times 10 \text{ mL}$ ) to afford light brown solids which were freeze dried for 24 h. The polymers were ground with a mortar and pestle and passed through a size-30 mesh sieve and stored in a desiccator for further use. A general illustration of the synthetic route for the FL-PFP terpolymer is illustrated in Scheme 1, along with the binary polymer (PFP) that does not contain TPE. The synthesis of the porous framework polymer (PFP) is described in the ESI, as described in Section S1.†

### Methods

Infrared spectroscopy was performed on a Bio-Rad FTS-40 spectrophotometer to yield diffuse reflectance infrared Fourier transform (DRIFT) spectra. Samples weighing *ca.* 5 mg were mixed with 10 mg of spectroscopic-grade KBr and corrected relative to a background KBr spectrum in reflectance mode. The spectral resolution was  $4 \text{ cm}^{-1}$  over the  $400\text{--}4000 \text{ cm}^{-1}$  region. The intensity of the spectra were normalized by the IR band of  $\beta$ -CD at  $1072 \text{ cm}^{-1}$ .

Thermogravimetric analysis (TGA) curves were recorded on a Q50 TA Instrument analyzer with aluminum sample pans. The sample in the pan was heated to  $308^\circ\text{C}$  and allowed to equilibrate for 5 min prior to heating at  $5^\circ\text{C min}^{-1}$  up to  $500^\circ\text{C}$  in a nitrogen atmosphere.





**Scheme 1** General illustration of the cross-linking of  $\beta$ -CD with diisocyanate linker (DL) is shown for the binary porous framework polymer (A) and the terpolymer system (B) that incorporates the fluorescent reporter unit (TPE).

The specific BET surface area (SA) of the polymer materials was measured using a Micromeritics ASAP 2020 (ver. 3.04).  $N_2$  gas adsorption-desorption isotherms were used to estimate BET SA accuracy to  $\pm 5\%$ . Powdered samples (*ca.* 1 g) were degassed at 120  $^{\circ}\text{C}$  for 24 h prior to isotherm analysis at  $-196^{\circ}\text{C}$ . Similar experimental conditions were used for  $\text{CO}_2$  adsorption-desorption analysis except that the isotherm analysis was carried out at 0  $^{\circ}\text{C}$ .

The fluorescence response of FL-PFP in the presence of variable guest concentration (TNP and NB) was measured using a TI Quantamaster spectrofluorometer. Fluorescence lifetimes were measured by time-correlated single-photon counting (TCSPC) and experiments were performed as described elsewhere.<sup>41</sup> The excitation light source used for fluorescence lifetime measurements was a Ti:sapphire laser (Mira, Coherent), which provided mode-locked pulses in the 700 to 1000 nm range. The 76 MHz pulse train was sampled using a pulse picker to provide excitation pulses at an acceptable repetition rate that was frequency doubled using a second harmonic generator. An excitation wavelength of 380 nm was chosen for measuring fluorescence decays. The instrument response function (IRF) was measured at the excitation wavelength using a Ludox scatterer, yielding an IRF with a width of *ca.* 100 ps. The time correlated single photon counting (TCSPC) technique was used to collect fluorescence decay curves with a minimum of 10k counts accumulated in the peak channel. Time-resolved fluorescence decay curves were analyzed by deconvolution of the observed decay traces with the IRF to obtain the intensity decay function represented as a sum of discrete exponentials:

$$I(t) = \sum_i \alpha_i \exp\left(-\frac{t}{\tau_i}\right) \quad (1)$$

$I(t)$  is the fluorescence intensity at time,  $t$ , and  $\alpha_i$  is the amplitude of the  $i^{\text{th}}$  lifetime, where  $\sum_i \alpha_i = 1$ . The goodness-of-fit to

the experimental data was evaluated by considering the reduced chi-squared values, along with an analysis of the statistical randomness of the weighted residuals.

## Fluorescence turn-off experiment

A stock solution of TNP and NB were prepared and diluted to make aqueous solutions that ranged between 0.05  $\mu\text{M}$  to 300  $\mu\text{M}$  in a 10 mM Tris-HCl buffer (pH 8). 5 mg of the fluorescent-based polymer was mixed with an aqueous solution containing known concentration of the TNP, where the total volume was 1 mL. The mixture was equilibrated with a horizontal shaker (250 rpm) for 5 min at 22  $^{\circ}\text{C}$ , centrifuged, filtered and freeze dried for 2 h to obtain a product in powder form composed of the fluorescence-based polymer bound to the explosive. The sample was analyzed using the fluorescence spectrophotometer in the wavelength range from 390 nm to 650 nm with an excitation wavelength of 380 nm.

## Results and discussion

The current study was focused on the development of a porous terpolymer that contains a fluorescent-based reporter unit (TPE) and  $\beta$ -CD *via* cross-linking (*cf.* Scheme 1). The terpolymer is a versatile host material with good structural stability and permanent porosity for the uptake and detection of nitroarenes, VOCs, or other gases. In contrast to the conventional approach of “turn-on” fluorescence detection, the method employed herein uses a modality employing fluorescence turn-off,<sup>8–13,17,18</sup> where TNP was used as a model electron deficient nitroarene for the sorption process. The materials characterization of the cross-linked polymers (PFP) and a terpolymer that contains TPE (FL-PFP) involved methods such as TGA, spectroscopy (FT-IR, NMR, and SEM) and gas adsorption isotherms that employ  $\text{CO}_2$  and  $\text{N}_2$  backfill gases.

### FTIR spectroscopy results

Fig. 1A depicts the IR spectra of native  $\beta$ -CD, DL, TPE, PFP and FL-PFP. The disappearance of the broad characteristic absorption peak of the isocyanato group ( $\text{N}=\text{C}=\text{O}$ ) at 2270  $\text{cm}^{-1}$  of PFP and FL-PFP provides support that cross-linking of  $\text{N}=\text{C}=\text{O}$  with  $\beta$ -CD furnished an amide linkage ( $-\text{CONH}-$ ). The binary (PFP) and terpolymer FL-PFP share similar spectral signatures to that of the individual components ( $\beta$ -CD, DL, TPE). The foregoing confers successful cross-linking as shown by the formation of the carbamate linkage. This is supported by the amide signature at 1647  $\text{cm}^{-1}$  and N-H stretching band at 1530–1541  $\text{cm}^{-1}$ . A decrease in the intensity of the C-O vibrational band at 1030  $\text{cm}^{-1}$  for  $\beta$ -CD is noted relative to the FL-PFP polymer. This is due to higher cross-linking ratios used in the polymerization resulting in the reaction of all the 21 available  $-\text{OH}$  groups on  $\beta$ -CD, as supported by the broad  $-\text{O}-\text{H}$  stretch at 3600  $\text{cm}^{-1}$  becomes narrow and shifts to lower frequency as evidenced by an N-H stretching band (3400  $\text{cm}^{-1}$ ). It is noteworthy that the polymer retains the structural rigidity of the diisocyanate cross-linker and the TPE unit. IR spectral evidence is provided by the stretching vibration of an aromatic group between 1604–1475  $\text{cm}^{-1}$  and the out-of-plane bending (832–600  $\text{cm}^{-1}$ ). To complement the IR results,  $^{13}\text{C}$  solids NMR spectra were obtained (*cf.* ESI, Fig. S1†). The NMR spectra for







Fig. 1 (A) FT-IR spectra of native  $\beta$ -CD (1), DL (2), TPE (3), PFP (4) and FL-PFP (5), (B) SEM image of PFP, (C) SEM image of FL-PFP, (D) DTA profiles (native  $\beta$ -CD, PFP and FL-PFP) for, (E)  $N_2$  adsorption-desorption isotherm for FL-PFP at  $-196^\circ\text{C}$  and (F)  $\text{CO}_2$  adsorption-desorption isotherm for FL-PFP at  $0^\circ\text{C}$ .

the polymers (PFP and FL-PFP) provide further evidence of cross-linking and the amorphous nature of these materials.

### TGA results

Fig. 1D shows the thermogram (TGA) results for native  $\beta$ -CD, PFP, and FL-PFP polymers. The results are plotted as the derivative weight loss/ $^\circ\text{C}$  vs. temperature (DTA) showing the degradation profiles of  $\beta$ -CD and the polymer materials. Two thermal events are observed where the process between  $50$ – $120^\circ\text{C}$  relates to the loss of adsorbed water and solvents. The thermal events for the polymers between  $350$ – $385^\circ\text{C}$  may relate to cleavage of the cross-links and/or breakdown of the polysaccharide framework.<sup>42</sup> The decomposition profile of the FL-PFP is broader in nature with evidence of greater thermal stability over native  $\beta$ -CD, as anticipated for such urethane based CD polymers.<sup>43</sup> The greater decomposition temperature of FL-PFP over  $\beta$ -CD is paralleled by the greater stabilization due to cross-linking as reported by Mohamed *et al.* for urethanes

that contain  $\beta$ -CD.<sup>43</sup> The polymer composition may be inferred from the relative peak areas of the deconvoluted DTA profile are in good general agreement with the FT-IR spectral results Fig. 1A. This includes the formation of the carbamate linkage due to cross-linking and other spectral signatures ( $-\text{O}-\text{H}$ ,  $\text{C}-\text{O}-\text{C}$  and  $\text{N}=\text{C}=\text{O}$ ) that provide additional evidence of cross-linking.

### SEM results

Fig. 1B and C illustrate the SEM images of PFP and FL-PFP polymer materials. The respective polymer surfaces reveal a combination of smooth, uniform and rod-like features that resemble linear dendrites. The mesh-like surface topography also reveals evidence of the porous polymer framework structure that is further supported by the nitrogen adsorption and BET results (*cf.* Fig. 1E and S2 of ESI†).  $\beta$ -CD-based polymers (PFP and FL-PFP) with greater cross-linking result in the formation of rigid materials with a dendritic morphology. The SEM results are consistent with the effects of cross-linking that account for changes in surface functionality and alteration of the polarity of the polymer, in agreement with the relative water insolubility of these polymers in aqueous media.

### Gas adsorption results

Fig. 1E shows the  $N_2$  adsorption-desorption isotherms for the FL-PFP polymer and Fig. S2 in the ESI† for PFP. The adsorption and desorption profiles of each polymer show typical characteristics of mesoporous materials, as noted for Type I isotherm profiles. The  $\text{H}_2$  type hysteresis loop<sup>44</sup> relates to the presence of an interconnected pore network. The BET SA estimate for the FL-PFP systems with  $N_2$  vary from  $100$ – $150\text{ m}^2\text{ g}^{-1}$  and show parallel agreement with the isotherm results for cross-linked CDs reported by Mohamed *et al.*<sup>45</sup> Alsbaiee *et al.*<sup>32</sup> reported that polymers with a greater SA correlate with systems prepared at higher levels of cross-linker ( $1 : 10 : 2$   $\beta$ -CD : DL : TPE). Other studies report greater SA for aromatic urethane polymers, while lower BET SA is evident for polymers obtained using flexible aliphatic cross-linker units.<sup>46</sup> The use of bulky and rigid connector units such as DL and TPE contribute to more rigid frameworks over that of aliphatic cross-linkers. As well, the variable steric bulk is known to influence the textural porosity of such polymers since the accessibility of  $\beta$ -CD inclusion and interstitial sites vary according to the nature of the cross-linker and its composition. The BET SA estimated from  $N_2$  isotherms for the FL-PFP system herein exceed that for other related CD-based cross-linked urethanes reported elsewhere.<sup>45</sup> The presence of TPE similarly contributes to structural rigidity and steric bulk adjacent to the  $\beta$ -CD sites of the polymer framework, in agreement with the SEM results (*cf.* Fig. 1B and C).

Fig. 1F shows the  $\text{CO}_2$  adsorption-desorption isotherms for FL-PFP and Fig. S3 in the ESI† for PFP. The FL-PFP and PFP systems have lower uptake of  $\text{CO}_2$  ( $20$ – $30\text{ m}^2\text{ g}^{-1}$ ) relative to  $N_2$  gas, in agreement with the larger molar volume and polarizability of  $\text{CO}_2$ . The  $-\text{OH}$  group accessibility of the CD moiety and amide groups of the linkage sites are inferred to play a role in  $\text{CO}_2$  adsorption due to its role in hydrogen bonding.  $\text{CO}_2$  uptake



was previously reported for lysinate salts,<sup>47</sup> where the amine sites play a key role in stabilizing Lewis acid–base interactions in complex formation.<sup>47,48</sup> Polymers with greater cross-linking have lower –OH group accessibility, in agreement with the IR results.<sup>49,50</sup> The role of the amide linkage may serve as a suitable adsorption site for CO<sub>2</sub> according to recent studies on the uptake of CO<sub>2</sub> in chitosan biopolymers.<sup>48</sup> The absence of the –OH band in the FT-IR spectra *ca.* 3400 cm<sup>−1</sup> is evident due to the effects of cross-linking. By contrast N<sub>2</sub> has smaller molar volume relative to CO<sub>2</sub>, where the adsorption sites are inferred to be nonspecific, in accordance with the offset in BET SA estimates. While gas adsorption provides insight on the textural properties, the use of solution-based adsorption provides complementary SA results according to the nature of the adsorbate and the solvent. A recent study has shown that nitrophenols with variable hydrophile–lipophile balance (HLB) can be adsorbed at inclusion *versus* interstitial domains of epichlorohydrin cross-linked materials that contain β-CD.<sup>51</sup> This can be understood since the interstitial domains that contain epichlorohydrin may possess greater hydrophile character over urethane linkages that contain lipophile cross-linker units such as TPE. As well, polysaccharide materials undergo solvent swelling in water, where judicious selection of adsorbate such as nitroarenes<sup>42</sup> with variable electron deficiency can provide insight on the structural characterization and the fluorescence quenching mechanism, as described below.

### Fluorescence properties of FL-PFP

The fluorescence “turn-off” properties of the FL-PFP polymer was studied using model nitroarenes (TNP and NB). The fluorescence emission intensity of the FL-PFP was observed to vary at different concentration levels of TNP and NB. An increase in the levels of TNP resulted in decreased emission intensity as shown in Fig. 2A. At higher levels of TNP, complete fluorescence “turn-off” was observed from the TPE fluorophore linker of the polymer framework. Since FL-PFP contains two accessible sites, the formation of a complex in the ground state is consistent with the above results. Based on the molecular size of TNP and known

stability of the β-CD/TNP complex, complexes may be formed with the inclusion and interstitial binding sites of the terpolymer. Collisional and static quenching are likely, as evidenced by the positive curvature noted in the S–V plots (*cf.* Inset of Fig. 2C and D) for the fluorescence emission of FL-PFP at variable nitroarene concentration. Similar trends in fluorescence emission was noted for poly(*p*-phenylene-butadiynylene)s and poly(*p*-phenylene-ethynylene)s, where the curvature of the S–V plot was attributed to decay contributions from collisional and static quenching.<sup>20</sup>

The interaction of the nitroarenes at the accessible sites of FL-PFP likely involve electrostatic, hydrophobic,  $\pi$ – $\pi$ , and hydrogen bonding interactions with the dual binding sites of the polymer. The phenyl ring, and phenolate anion of TNP enable favourable electrostatic,  $\pi$ – $\pi$ , and hydrogen bonding donor–acceptor interactions with the interstitial TPE site of FL-PFP, along with the amide linkages.<sup>8,9,17,18</sup> A comparison of the quenching profiles of both TNP and NB reveal that the interaction between TNP and FL-PFP is greatly enhanced by the incremental electron withdrawing effect of the –NO<sub>2</sub> substituents. The variable Lewis basicity or HLB character of the nitroarenes are likely to contribute to the variable binding affinity with the adsorption sites of FL-PFP, aside from their respective hydration properties in such host–guest systems.<sup>28,52–54</sup> The fluorescence quenching of FL-PFP by TNP is more pronounced over NB, as shown by visual differences in fluorescence quenching properties, where NB shows negligible quenching behaviour. By contrast, TNP quenches *ca.* 50% of the observed fluorescence of FL-PFP at *ca.* 50 nM. Fig. 3 shows a plausible mechanism for the quenching of the fluorescence of FL-PFP by TNP that can be understood by the formation of a donor–acceptor (D–A) complex between TPE and the nitroarene guest. The D–A complex is anticipated to quench the  $\pi \rightarrow \pi^*$  transition, in line with the results presented in Fig. 2.

To further understand the quenching response to variable levels of TNP, the quantum yield ( $\phi$ ) of FL-PFP and the fluorescence lifetime of the FL-PFP/TNP system at variable concentration was studied. The estimated value for  $\phi$  was  $0.399 \pm 0.06$  with reference to quinine sulphate. The lifetime ( $\tau$ ) of the FL-PFP polymer in the absence and presence of different levels of TNP was constant using an excitation wavelength at 380 nm. The resulting fluorescence decay trace was fitted to a bi-exponential decay function to yield an estimated value for  $\tau = 3.88$  ns. However, the bi-exponential decay function did not

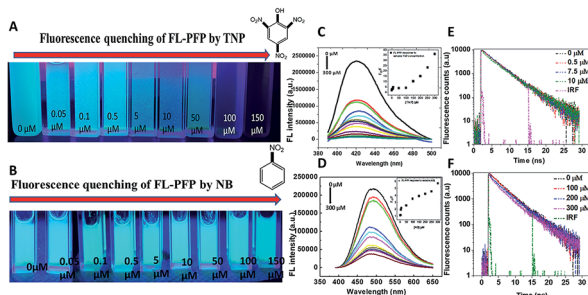


Fig. 2 (A and B) Visual observation of the fluorescence quenching response of FL-PFP at variable adsorbate concentration ([TNP] and [NB]) in a 10 mM Tris–HCl buffer (pH 8), (C and D) fluorescence quench at different values of [TNP] and [NB], where the inset shows the non-linear S–V plots that illustrate different quenching mechanisms, (E) time-resolved fluorescence decay of the FL-PFP system at different TNP levels (mono-exponential fit) and (F) time-resolved decay of the FL-PFP system at different TNP concentration (bi-exponential fit).

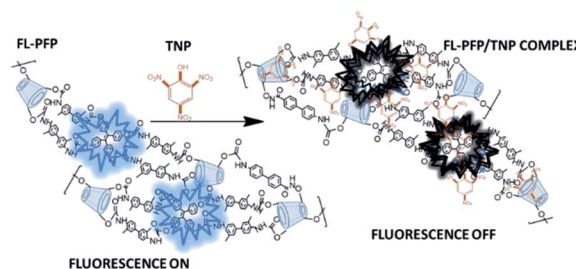


Fig. 3 An illustration of the “on-off” fluorescence quenching mechanism for the FL-PFP/TNP system, where complexes between TPE and TNP at the interstitial sites are likely to induce quenching along with inclusion binding at the CD cavity sites.



**Table 1** Decay parameters of PFP-FL polymer in the presence of TNP ( $\lambda_{\text{excitation}} = 380 \text{ nm}$ )<sup>a</sup>

[TNP] $\mu\text{M}$	$\lambda_{\text{em}}$ (nm)	$\tau_1$ (ns)	$\tau_2$ (ns)	$a_1$ (%)	$a_2$ (%)	$\chi^2$
0	420	$3.88 \pm 0.02$	—	1	—	1.00
0.5	420	$3.70 \pm 0.01$	—	1	—	1.00
7.5	420	$3.62 \pm 0.01$	—	1	—	1.02
10	420	$3.53 \pm 0.01$	—	1	—	1.03
100	420	$3.67 \pm 0.02$	$0.126 \pm 0.01$	0.714	0.285	1.01
200	420	$3.60 \pm 0.01$	$0.125 \pm 0.01$	0.701	0.298	1.01
300	420	$3.53 \pm 0.01$	$0.0821 \pm 0.01$	0.944	0.0559	1.02

<sup>a</sup> Standard deviation is given for the lifetimes, where the chi-square ( $\chi^2$ ) term for the best fit is listed for a mono- or bi-exponential fit function.

provide a suitable best-fit at lower TNP levels; whereas a single-exponential function provided a better best-fit profile. The fluorescence decay results suggest two possible mechanisms: (1) diffusion of the TNP onto the surface accessible interstitial domains of FL-PFP, and (2) the complexation of the TNP with the FL-PFP in the ground state at multiple binding sites (interstitial and inclusion domains). The time resolved fluorescence decay results for FL-PFP in the presence of variable TNP levels are shown in Fig. 2E, F and Table 1.

## Conclusions

In this study, a one pot synthesis was used to design a porous fluorescence-based polymer (FL-PFP) containing  $\beta$ -CD. FL-PFP displays with unique photophysical and textural properties are responsive to the binding of nitroarene guests. The rigidity and mesoporous structure of FL-PFP results due to contribution of the  $\beta$ -CD inclusion sites and rigid subunits (TPE and DL) that constitute the polymer framework, in accordance with the gas adsorption results, and the ability to form stable host-guest complexes with nitroarenes (TNP and NB) in aqueous media. A facile fluorescence “turn-off” method was developed for the sensitive detection of TNP in aqueous solution that reveals the role of dual binding sites (inclusion and interstitial),<sup>55</sup> in accordance with time-resolved fluorescence decay lifetime results. The accessibility of dual binding sites of the FL-PFP material facilitate controlled adsorption and detection of TNP, as evidenced by dynamic and static fluorescence quenching results. The details of the mechanism for this phenomena is the subject of ongoing research that will explore further synthetic modification and potential for molecular selective detection of structurally related guest systems.<sup>6,8,10,12,14,17,18,56</sup> The significance of this work relates to the design of engineered materials and the demonstration of an “on-off” fluorescence detection modality for model nitroarene compounds. Further studies are underway to develop sensor materials with enhanced molecular recognition properties toward environmental contaminants for field-based applications.<sup>6,8–11,16–19,34,57,58</sup>

## Conflicts of interest

The authors declare no conflicts of interest.

## Acknowledgements

The authors gratefully acknowledge support provided by the University of Saskatchewan and the Beijing Institute of Technology through the award of an IFPRG grant. L. D. W. acknowledges the support by the Government of Canada through the Natural Sciences and Engineering Research Council of Canada (Discovery Grant Number: RGPIN 2016-06197). M. K. D. acknowledges Mitacs for a Globalink award to support international research at the Beijing Institute of Technology (Beijing, China).

## Notes and references

- 1 Y. Salinas, R. Martínez-Máñez, M. D. Marcos, F. Sancenón, A. M. Costero, M. Parra and S. Gil, Optical Chemosensors and Reagents to Detect Explosives, *Chem. Soc. Rev.*, 2012, **41**, 1261–1296.
- 2 M. E. Germain and M. J. Knapp, Optical Explosives Detection: From Color Changes to Fluorescence Turn-On, *Chem. Soc. Rev.*, 2009, **38**, 2543–2555.
- 3 S. D. Richardson, Water Analysis, *Anal. Chem.*, 2001, **73**, 2719–2734.
- 4 S. S. R. Dasary, A. K. Singh, D. Senapati, H. Yu and P. C. Ray, Gold Nanoparticle Based Label-Free SERS Probe for Ultrasensitive and Selective Detection of Trinitrotoluene, *J. Am. Chem. Soc.*, 2009, **131**, 13806–13812.
- 5 K. E. Brown, M. T. Greenfield, S. D. McGrane and D. S. Moore, Advances in Explosives Analysis-Part II: Photon and Neutron Methods, *Anal. Bioanal. Chem.*, 2016, **408**(1), 49–65.
- 6 F. Cheng, X. An, C. Zheng and S. Cao, Green Synthesis of Fluorescent Hydrophobic Carbon Quantum Dots and Their Use for 2,4,6-Trinitrophenol Detection, *RSC Adv.*, 2015, **5**(113), 93360–93363.
- 7 Y. Ma, S. Huang, M. Deng and L. Wang, White Upconversion Luminescence Nanocrystals for the Simultaneous and Selective Detection of 2,4,6-Trinitrotoluene and 2,4,6-Trinitrophenol, *ACS Appl. Mater. Interfaces*, 2014, **6**, 7790–7796.
- 8 Y. Ma, H. Li, S. Peng and L. Wang, Highly Selective and Sensitive Fluorescent Paper Sensor for Nitroaromatic Explosive Detection, *Anal. Chem.*, 2012, **84**(19), 8415–8421.
- 9 S. S. Nagarkar, B. Joarder, A. K. Chaudhari, S. Mukherjee and S. K. Ghosh, Highly Selective Detection of Nitro Explosives by a Luminescent Metal-Organic Framework, *Angew. Chem., Int. Ed.*, 2013, **52**(10), 2881–2885.
- 10 K. Zhang, H. Zhou, Q. Mei, S. Wang, G. Guan, R. Liu, J. Zhang and Z. Zhang, Instant Visual Detection of Trinitrotoluene Particulates on Various Hybrid, *J. Am. Chem. Soc.*, 2011, **133**, 8424–8427.
- 11 Y. Wang and Y. Ni, Molybdenum Disulfide Quantum Dots as a Photoluminescence Sensing Platform for 2,4,6-Trinitrophenol Detection, *Anal. Chem.*, 2014, **86**, 7463–7470.
- 12 J. Li, C. E. Kendig and E. E. Nesterov, Chemosensory Performance of Molecularly Imprinted Fluorescent





- Conjugated Polymer Materials, *J. Am. Chem. Soc.*, 2007, **129**(51), 15911–15918.
- 13 C. Xie, B. Liu, Z. Wang, D. Gao, G. Guan and Z. Zhang, Molecular Imprinting at Walls of Silica Nanotubes for TNT Recognition, *Anal. Chem.*, 2008, **80**, 437–443.
  - 14 E. R. Goldman, I. L. Medintz, J. L. Whitley, A. Hayhurst, A. R. Clapp, H. T. Uyeda, J. R. Deschamps, M. E. Lassman and H. Mattoussi, A Hybrid Quantum Dot-Antibody Fragment Fluorescence Resonance Energy Transfer-Based TNT Sensor, *J. Am. Chem. Soc.*, 2005, **127**(18), 6744–6751.
  - 15 Y. Jiang, H. Zhao, N. Zhu, Y. Lin, P. Yu and L. Mao, A Simple Assay for Direct Colorimetric Visualization of Trinitrotoluene at Picomolar Levels Using Gold Nanoparticles, *Angew. Chem., Int. Ed.*, 2008, **47**(45), 8601–8604.
  - 16 S. Wang, Q. Wang, X. Feng, B. Wang and L. Yang, Explosives in the Cage: Metal–Organic Frameworks for High-Energy Materials Sensing and Desensitization, *Adv. Mater.*, 2017, **29**, 1–17.
  - 17 Y. Guo, X. Feng, T. Han, S. Wang, Z. Lin, Y. Dong and B. Wang, Tuning the Luminescence of Metal–Organic Frameworks for Detection of Energetic Heterocyclic Compounds, *J. Am. Chem. Soc.*, 2014, **136**(44), 15485–15488.
  - 18 M. Rong, L. Lin, X. Song, T. Zhao, Y. Zhong, J. Yan, Y. Wang and X. Chen, A Label-Free Fluorescence Sensing Approach for Selective and Sensitive Detection of 2,4,6-Trinitrophenol (TNP) in Aqueous Solution Using Graphitic Carbon Nitride Nanosheets, *Anal. Chem.*, 2015, **87**(2), 1288–1296.
  - 19 J. S. Yang and T. M. Swager, Fluorescent Porous Polymer Films as TNT Chemosensors: Electronic and Structural Effects, *J. Am. Chem. Soc.*, 1998, **120**, 11864–11873.
  - 20 D. Zhao and T. M. Swager, Sensory Responses in Solution vs. Solid State: A Fluorescence Quenching Study of Poly(iptycenebutadiynylene)s, *Macromolecules*, 2005, **38**, 9377–9384.
  - 21 T. Ogoshi and A. Harada, Chemical Sensors Based on Cyclodextrin Derivatives, *Sensors*, 2008, **8**, 4961–4982.
  - 22 J. W. Steed and J. L. Atwood, *Supramolecular Chemistry*, John Wiley & Sons, Ltd, Chichester, West Sussex, 2nd edn, 2009.
  - 23 G. Wenz, Cyclodextrins as Building Blocks for Supramolecular Structures and Functional Units, *Angew. Chem., Int. Ed. Engl.*, 1994, **33**, 803–822.
  - 24 G. Crini and M. Morcellet, Synthesis and Applications of Adsorbents Containing Cyclodextrins, *J. Sep. Sci.*, 2002, **25**, 789–813.
  - 25 M. H. Mohamed, L. D. Wilson, J. V. Headley and K. M. Peru, Thermodynamic Properties of Inclusion Complexes between  $\beta$ -Cyclodextrin and Naphthenic Acid Fraction Components, *Energy Fuels*, 2015, **29**, 3591–3600.
  - 26 G. Crini, Review: A History of Cyclodextrins, *Chem. Rev.*, 2014, **114**, 10940–10975.
  - 27 G. Wenz, Inclusion Polymers, *J. Am. Chem. Soc.*, 2009, **131**, 17994.
  - 28 N. Morin-Crini, P. Winterton, S. Fourmentin, L. D. Wilson, É. Fenyvesi and G. Crini, Water-Insoluble  $\beta$ -Cyclodextrin-epichlorohydrin Polymers for Removal of Pollutants from Aqueous Solutions by Sorption Processes Using Batch Studies: A Review of Inclusion Mechanisms, *Prog. Polym. Sci.*, 2018, **78**, 1–23.
  - 29 M. V. Rekharsky and Y. Inoue, Complexation Thermodynamics of Cyclodextrins, *Chem. Rev.*, 1998, **98**, 1875–1918.
  - 30 J. Szejtli, *Cyclodextrins and Their Inclusion Complexes*, Akadémiai Kiadó, Budapest, 1982.
  - 31 H. Li, B. Meng, S.-H. Chai, H. Liu and S. Dai, Hyper-Crosslinked  $\beta$ -Cyclodextrin Porous Polymer: An Adsorption-Facilitated Molecular Catalyst Support for Transformation of Water-Soluble Aromatic Molecules, *Chem. Sci.*, 2016, **7**, 905–909.
  - 32 A. Alsbaiee, B. J. Smith, L. Xiao, Y. Ling, D. E. Helbling and W. R. Dichtel, Rapid Removal of Organic Micropollutants from Water by a Porous  $\beta$ -Cyclodextrin Polymer, *Nature*, 2016, **529**, 190–194.
  - 33 T. Tanabe, K. Touma, K. Hamasaki and A. Ueno, Immobilized Fluorescent Cyclodextrin on a Cellulose Membrane as a Chemosensor for Molecule Detection, *Anal. Chem.*, 2001, **73**, 3126–3130.
  - 34 G. Liang, F. Ren, H. Gao, Q. Wu, F. Zhu and B. Zhong Tang, Bioinspired Fluorescent Nanosheets for Rapid and Sensitive Detection of Organic Pollutants in Water, *ACS Sens.*, 2016, **1**, 1272–1278.
  - 35 A. Qin, J. W. Y. Lam, F. Mahtab, C. K. W. Jim, L. Tang, J. Sun, H. H. Y. Sung, I. D. Williams and B. Z. Tang, Pyrazine Luminogens with “free” and “locked” Phenyl Rings: Understanding of Restriction of Intramolecular Rotation as a Cause for Aggregation-Induced Emission, *Appl. Phys. Lett.*, 2009, **94**(25), 2007–2010.
  - 36 H. T. Feng, J. H. Wang and Y. S. Zheng,  $\text{CH}_3$ - $\pi$  Interaction of Explosives with Cavity of a TPE Macrocycle: The Key Cause for Highly Selective Detection of TNT, *ACS Appl. Mater. Interfaces*, 2014, **6**(22), 20067–20074.
  - 37 D. Li, J. Liu, R. T. K. Kwok, Z. Liang, B. Z. Tang and J. Yu, Supersensitive Detection of Explosives by Recyclable AIE Luminogen-Functionalized Mesoporous Materials, *Chem. Commun.*, 2012, **48**(57), 7167.
  - 38 M. Wang, G. Zhang, D. Zhang, D. Zhu and B. Z. Tang, Fluorescent Bio/chemosensors Based on Silole and Tetraphenylethene Luminogens with Aggregation-Induced Emission Feature, *J. Mater. Chem.*, 2010, **20**(10), 1858.
  - 39 Y. Hong, J. W. Y. Lam and B. Z. Tang, Aggregation-Induced Emission, *Chem. Soc. Rev.*, 2011, **40**(11), 5361.
  - 40 H. T. Feng and Y. S. Zheng, Highly Sensitive and Selective Detection of Nitrophenolic Explosives by Using Nanospheres of a Tetraphenylethylene Macrocycle Displaying Aggregation-Induced Emission, *Chem.-Eur. J.*, 2014, **20**(1), 195–201.
  - 41 N. K. Joshi, A. M. Polgar, R. P. Steer and M. F. Paige, Photochemical & Photobiological Sciences White Light Generation Using Förster Resonance Energy Transfer between 3-Hydroxyisoquinoline and Nile Red, *Photochem. Photobiol. Sci.*, 2016, **15**(15), 597–706.
  - 42 M. H. Mohamed, L. D. Wilson, J. V. Headley and K. M. Peru, Investigation of the Sorption Properties of  $\beta$ -Cyclodextrin-



- Based Polyurethanes with Phenolic Dyes and Naphthenates, *J. Colloid Interface Sci.*, 2011, **356**, 217–226.
- 43 M. H. Mohamed, L. D. Wilson and J. V. Headley, Design and Characterization of Novel  $\beta$ -Cyclodextrin Based Copolymer Materials, *Carbohydr. Res.*, 2011, **346**, 219–229.
  - 44 K. S. W. Sing, D. H. Everett, R. A. W. Haul, L. Moscou, L. A. Pierotti, J. Rouquerol and T. Siemieniewska, International Union of Pure and Applied Chemistry Physical Chemistry Division Reporting Physisorption Data for Gas/soils Systems with Special Reference to the Determination of Surface Area and Porosity, *Pure Appl. Chem.*, 1985, **57**, 603–619.
  - 45 L. D. Wilson, M. H. Mohamed and J. V. Headley, Surface Area and Pore Structure Properties of Urethane-Based Copolymers Containing  $\beta$ -Cyclodextrin, *J. Colloid Interface Sci.*, 2011, **357**(1), 215–222.
  - 46 M. H. Mohamed, L. D. Wilson and J. V. Headley, Tuning the Physicochemical Properties of  $\beta$ -Cyclodextrin Based Polyurethanes via Cross-Linking Conditions, *Microporous Mesoporous Mater.*, 2015, **214**, 23–31.
  - 47 Y. Zhang, S. Zhang, X. Lu, Q. Zhou, W. Fan and X. P. Zhang, Dual Amino-Functionalised Phosphonium Ionic Liquids for CO<sub>2</sub> Capture, *Chem.–Eur. J.*, 2009, **15**, 3003–3011.
  - 48 A. K. Qaroush, K. I. Assaf, S. K. Bardaweel, A. Al-Khateeb, F. Alsoubani, E. Al-Ramahi, M. Masri, T. Brück, C. Troll, B. Rieger, *et al.*, Chemisorption of CO<sub>2</sub> by Chitosan oligosaccharide/DMSO: Organic Carbamate-Carbonate Bond Formation, *Green Chem.*, 2017, **19**, 4305–4314.
  - 49 A. P. Katsoulidis and M. G. Kanatzidis, Phloroglucinol Based Microporous Polymeric Organic Frameworks with-OH Functional Groups and High CO<sub>2</sub> Capture Capacity, *Chem. Mater.*, 2011, **23**(7), 1818–1824.
  - 50 M. B. Yue, L. B. Sun, Y. Cao, Z. J. Wang, Y. Wang, Q. Yu and J. H. Zhu, Promoting the CO<sub>2</sub> Adsorption in the Amine-Containing SBA-15 by Hydroxyl Group, *Microporous Mesoporous Mater.*, 2008, **114**(1–3), 74–81.
  - 51 M. K. Danquah, R. Aruei and L. Wilson, Phenolic Pollutants Uptake Properties of Molecular Templated Polymers Containing  $\beta$ -Cyclodextrin, *J. Phys. Chem. B*, 2018, **122**(17), 4748–4757.
  - 52 N. Morin-Crini and G. Crini, Environmental Applications of Water-Insoluble  $\beta$ -Cyclodextrin-Epichlorohydrin Polymers, *Prog. Polym. Sci.*, 2013, **38**, 344–368.
  - 53 A. Harada, M. Furue and S. Nozakura, Cyclodextrin-Containing Polymers. Cooperative Effects in Catalysis and Binding, *Macromolecules*, 1976, **9**, 705–710.
  - 54 G. Crini, S. Bertini, G. Torri, A. Naggi, D. Sforzini, C. Vecchi, L. Janus, Y. Lekchiri and M. Morcellet, Sorption of Aromatic Compounds in Water Using Insoluble Cyclodextrin Polymers, *J. Appl. Polym. Sci.*, 1998, **68**, 1973–1978.
  - 55 N. Morin-Crini, P. Winterton, S. Fourmentin, L. D. Wilson, É. Fenyvesi and G. Crini, Water-Insoluble  $\beta$ -Cyclodextrin-Epichlorohydrin Polymers for Removal of Pollutants from Aqueous Solutions by Sorption Processes Using Batch Studies: A Review of Inclusion Mechanisms, *Prog. Polym. Sci.*, 2017, **78**, 1–23.
  - 56 V. de Zea Bermudez, L. D. Carlos, M. M. Silva and M. J. Smith, An Interesting Ligand for the Preparation of Luminescent Plastics: The Picrate Ion, *J. Chem. Phys.*, 2000, **112**(7), 3293–3313.
  - 57 B. Valeur, *Molecular Fluorescence: Principles and Applications*, Wiley-VCH, New York, 2012, vol. 8.
  - 58 J. R. Lakowicz, *Principle of Florescence Spectroscopy*, Kluwer Academic/Plenum Publishers, New York, 2nd edn, 1999.

